Supporting information for

Field-induced mononuclear cobalt(II) single-molecule magnet (SMM) based on a benzothiadiazole-*ortho*-vanillin ligand

Nataliya Plyuta,[a] Svitlana Petrusenko,[b] Vladimir N. Kokozay,[b] Thomas Cauchy,[a] Francesc Lloret,[c] Miguel Julve,[c] Joan Cano*[c] and Narcis Avarvari*[a]

[a] *Univ Angers, CNRS, MOLTECH-Anjou, SFR MATRIX, F-49000 Angers, France. E-mail: narcis.avarvari@univ-angers.fr*

[b] *Department of Inorganic Chemistry, Taras Shevchenko National University of Kyiv, Volodymyrska str. 64/13, Kyiv 01601, Ukraine*

[c] *Instituto de Ciencia Molecular (ICMol)/Departament de Química Inorgànica, Universitat de València, C/ Catedrático José Beltrán 2, 46980 Paterna (Valencia) (Spain). E-mail: Joan.Cano@uv.es*

Experimental section

General comments. All the reactions were carried out under ambient conditions with HPLC-grade solvents. Nuclear magnetic resonance spectra were recorded on a Bruker Avance DRX 300 spectrometer operating at 300 and 75 MHz for ^{1}H and ^{13}C, respectively. Chemical shifts are expressed in parts per million (ppm) downfield from external TMS. The following abbreviations (δ) are used: s, singlet; d, doublet; t, triplet; m, massif. MALDI-TOF MS spectra were done on a Bruker Biflex-IIITM apparatus, equipped with a 337 nm N_2 laser. Elemental analysis were recorded using a Flash 2000 Fisher Scientific Thermo Electron analyzer. The IR spectra were performed on an ATR Bruker Vertex 70 spectrophotometer in the range 4000-400 cm^{-1}. Signal intensities (height) are denoted by the following abbreviations: vs-very strong, s-strong, m-medium and w-weak.

X-Ray structure determinations

Details about data collection and solution refinement are given in Table S1. Single crystals of the compounds were mounted on glass fibre loops using a viscous hydrocarbon oil to coat the crystal and then transferred directly to a cold nitrogen stream for data collection. Data collection were mostly performed at 150 K on an Agilent Supernova with Cu Kα (λ = 1.54184 Å). The structures were solved by direct methods with the SIR92 program and refined against all F^2 values with the SHELXL-97 program[1] using the WinGX graphical user interface.[2] All non-H atoms were refined anisotropically. The hydrogen atoms were introduced at calculated positions (riding model) and included in the structure factor calculations but not refined.

Crystallographic data for the two structures have been deposited with the Cambridge Crystallographic Data Centre, deposition numbers CCDC 2128849 (HL) and 2128850 ($[CoL_2]\cdot CH_2Cl_2$). These data can be obtained free of charge from CCDC, 12 Union road, Cambridge CB2 1EZ, UK (e-mail: deposit@ccdc.cam.ac.uk or http://www.ccdc.cam.ac.uk).

Table S1 Crystal Data and Structure Refinement for HL and $[CoL_2]\cdot CH_2Cl_2$

Compound	HL	$[CoL_2]\cdot CH_2Cl_2$
Empirical formula	$C_{14}H_{11}N_3O_2S$	$C_{29}H_{22}Cl_2CoN_6O_4S_2$
Molecular weight	285.32	712.47
T (K)	150.00(10)	149.3(4)
Wavelength (Å)	1.54184	1.54184
Crystal system	Monoclinic	Triclinic
Space group	$P2_1/c$	*P*-1
a (Å)	12.5784(4)	11.0894(7)
b (Å)	5.23110(10)	12.3519(8)
c (Å)	19.7962(7)	13.0378(8)
α (deg)	90	90.231(5)
β (deg)	105.161(3)	111.019(6)
γ (deg)	90	114.765(6)
V (Å^3)	1257.23(7)	1488.43(18)
Z	4	2
D_c (g cm^{-3})	1.507	1.590
Abs. coeff. (mm^{-1})	2.343	7.887
Crystal size (mm^3)	0.15 x 0.09 x 0.07	0.10 x 0.05 x 0.04
θ (min/max)	3.641/72.176	3.694/73.777
Transmission (min/max)	0.80686/1.00000	0.63379/1.00000
Data collected/unique	4305/2405	10877/5673
Data/restraints/parameters	2405/0/183	5673/0/399
R (int)	0.0240	0.0800
GOF on F^2	1.051	1.028
final *R* indices[a] [$I > 2\sigma(I)$]	0.0293/0.0736	0.0734/0.1852
R indices (all data)	0.0342/0.0767	0.0964/0.2075
Largest maximum/minimum peak in final difference (e A^{-3})	0.263/-0.271	1.669/-1.822
CCDC number	2128849	2128850

[a] $R(F_o) = \Sigma||F_o| - |F_c||/\Sigma|F_o|$; $R_w(F_o^2) = [\Sigma[w(F_o^2 - F_c^2)^2]/\Sigma[w(F_o^2)^2]]^{1/2}$.

Compound HL

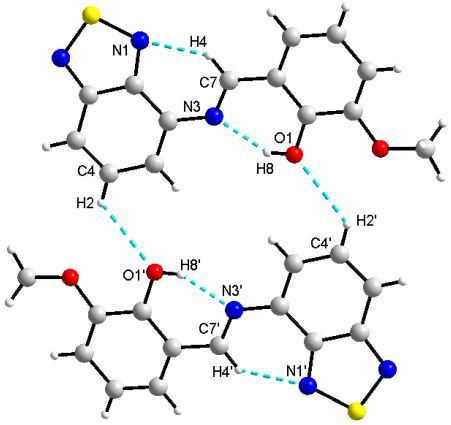

Fig. S1 Molecular structure of HL in the solid state highlighting the dimer formation upon the O1···H2'–C4' type interaction. [Symmetry code: (´) = 1–*x*, 1–*y*, 1–*z*].

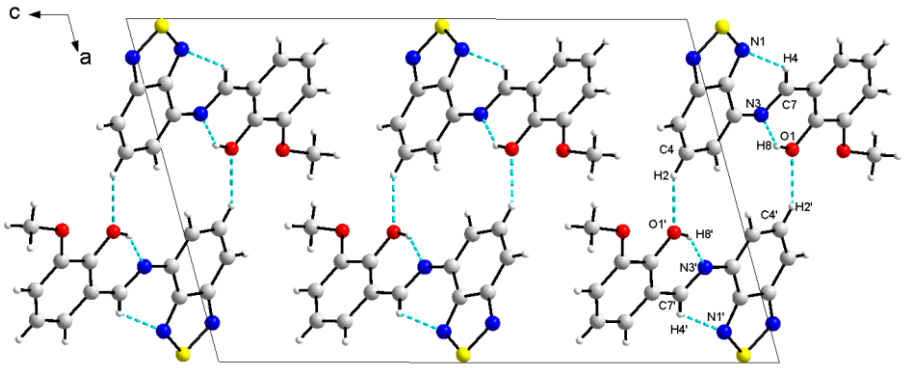

Fig. S2 Packing diagram of HL in the crystallographic *ac* plane.

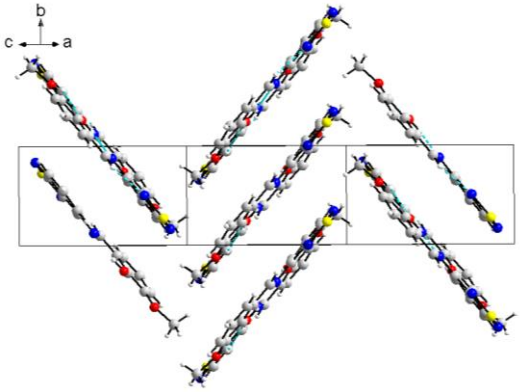

Fig. S3 View of the packing of HL.

Table S2 Hydrogen bonds and O···H-C type interaction parameters (Å, °) of compound HL

	A···H – D	**d(A···H), Å**	**d(A···D) , Å**	**∠ (D – H···A), °**
	N(1)···H(4) – C(7)	2.242	2.929	130.12
H**L**	N(3)···H(8) – O(1)	1.871	2.597	146.91
	O'(1)···H(2) – C(4)*	2.578	3.245	129.03

*Symmetry code: [a] = 1–*x*, 1–*y*, 1–*z*.

DFT calculations on compound HL

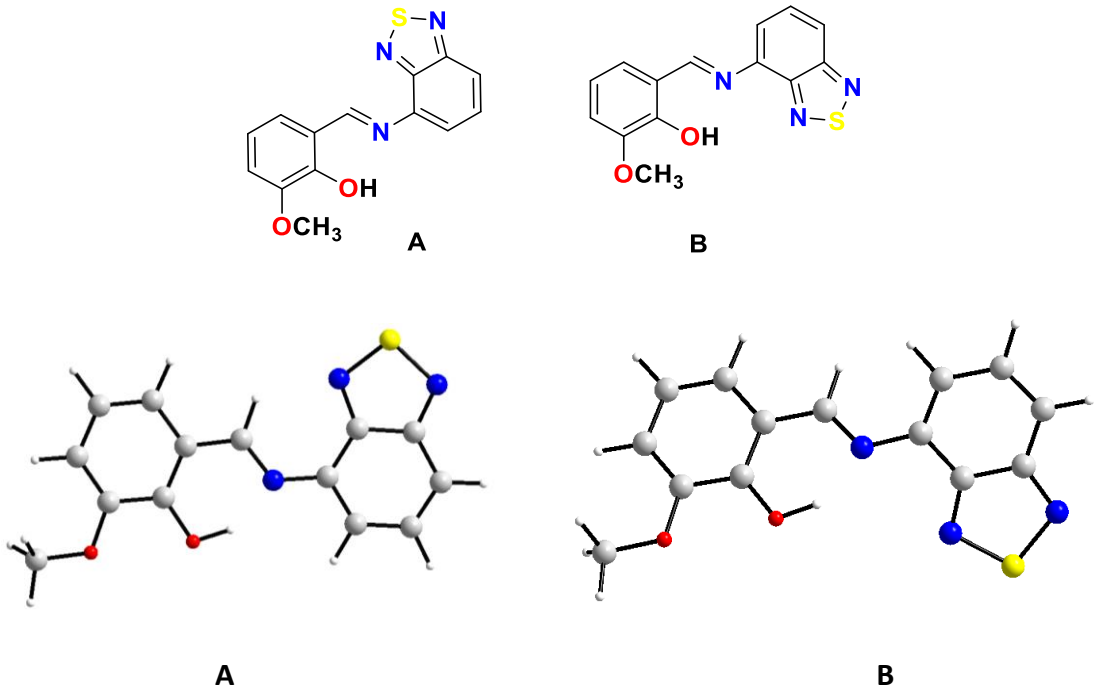

Fig. S4 The two equilibrium geometries **A** and **B** of HL in the *E* configuration.

Table S3 Converged Cartesian coordinates of calculated **A**-HL and **B**-HL

A-HL				**B**-HL			
S	4.0618	-1.9887	0	C	-2.8237	2.0102	-0.8391
N	2.5431	-1.3821	0.0001	C	-1.9431	1.0409	-0.3256
C	2.6565	-0.0574	0	C	-2.4424	-0.1864	0.1516
C	4.0321	0.3932	-0.0001	C	-3.8368	-0.4179	0.1128
N	4.9156	-0.601	0	C	-4.6781	0.5561	-0.3931
C	4.3517	1.772	-0.0001	C	-4.1737	1.7722	-0.8697
C	3.3156	2.6571	-0.0001	C	-0.53	1.3113	-0.2993
C	1.9659	2.2295	-0.0001	N	0.3228	0.47	0.1635
C	1.5883	0.9062	0	C	1.6687	0.7917	0.2503
N	0.2288	0.6369	0	C	2.6308	-0.2291	-0.0279
C	-0.2773	-0.5519	0.0001	C	4.0406	0.0527	0.0807
C	-1.7024	-0.7564	0.0001	C	4.4883	1.3353	0.4822
C	-2.5914	0.3367	0.0001	C	3.5429	2.2781	0.7579
C	-3.983	0.0908	0	C	2.1521	2.0137	0.6493
C	-4.4467	-1.2119	-0.0002	N	4.8107	-0.9909	-0.2184
C	-3.559	-2.295	-0.0001	S	3.7989	-2.2142	-0.6023
C	-2.2063	-2.0705	0	N	2.3583	-1.4709	-0.4089
O	-2.169	1.5935	0.0004	O	-1.6602	-1.1408	0.634
O	-4.7617	1.1944	0	O	-4.2327	-1.6162	0.5902
C	-6.1563	1.0097	-0.0002	C	-5.6097	-1.9058	0.5729
H	5.388	2.0837	-0.0002	H	5.5487	1.534	0.5688
H	3.5168	3.7223	-0.0002	H	3.8512	3.2659	1.0821
H	1.1763	2.972	-0.0001	H	1.4499	2.7921	0.9266
H	0.3528	-1.4414	0.0001	H	-0.2031	2.2733	-0.7126
H	-1.5052	-2.8982	0	H	-2.4165	2.9466	-1.2061
H	-3.9514	-3.3047	-0.0003	H	-4.8573	2.5152	-1.262
H	-5.5121	-1.4037	-0.0003	H	-5.7459	0.3807	-0.4241
H	-6.4929	0.4706	0.8931	H	-6.0102	-1.9035	-0.4474
H	-6.4927	0.4707	-0.8935	H	-6.1795	-1.1974	1.1853
H	-6.592	2.0072	0.0001	H	-5.7117	-2.9043	0.9941
H	-1.1691	1.5489	0.0006	H	-0.7214	-0.8159	0.5671

Complex $[CoL_2]\cdot CH_2Cl_2$

(a) **(b)**

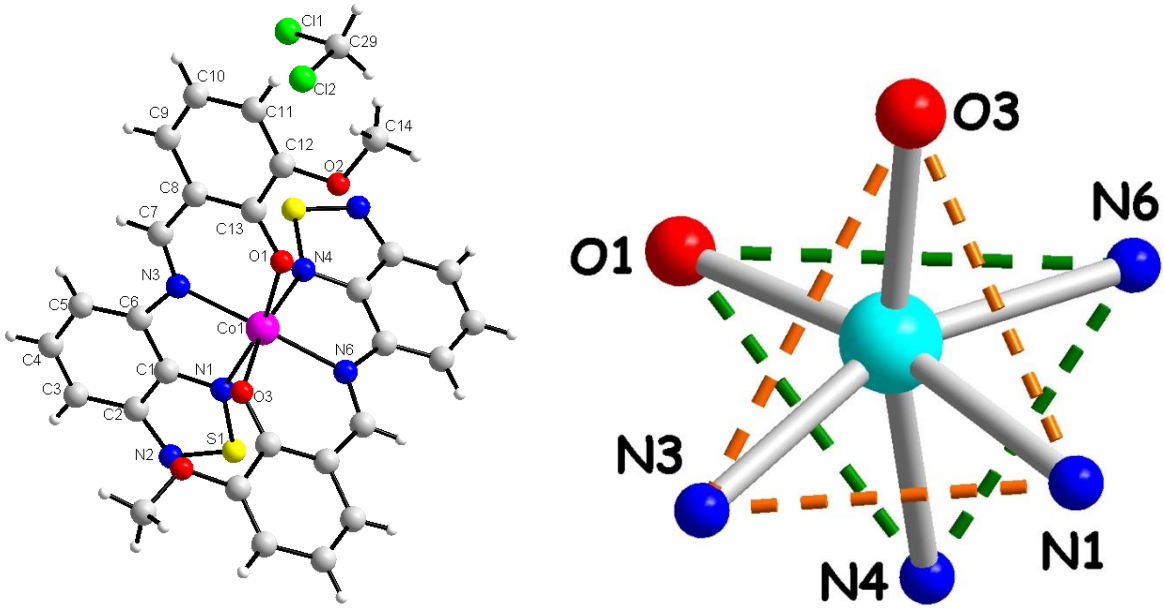

Fig. S5 Molecular structure of $[CoL_2]\cdot CH_2Cl_2$ in the solid state (a) and highlight on the coordination sphere of cobalt(II) (b).

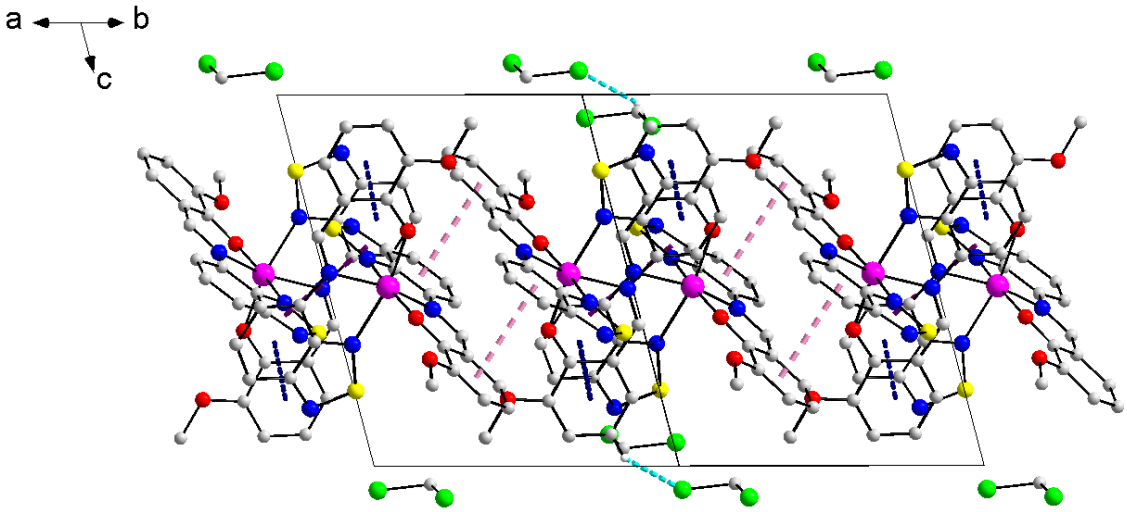

Fig. S6 A view of the packing diagram of $[CoL_2]\cdot CH_2Cl_2$ showing the π-π type interactions (dashed lines).

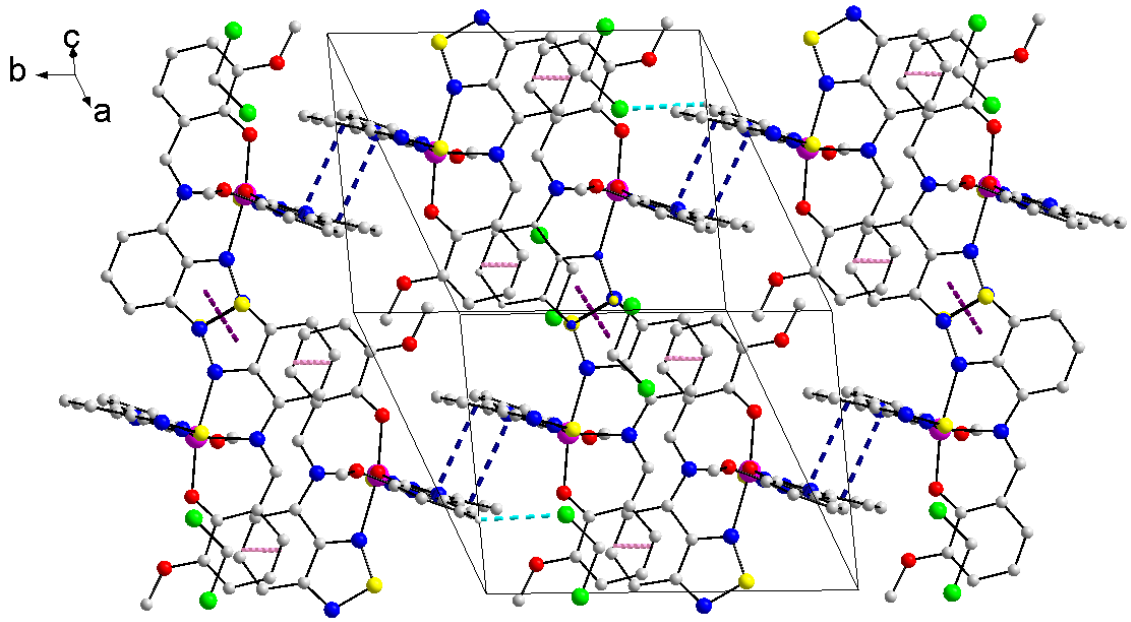

Fig. S7 Perspective view of the supramolecular assembly in $[CoL_2]\cdot CH_2Cl_2$: π···π phenolate-BTD rings 3.55 Å (pink), π···π phenolate-BTD rings 3.52 Å (blue), π···π TD-TD rings 3.67 Å (violet) and C–H···Cl type (light blue) interactions in the crystal packing.

Table S4 Selected bond distances (Å) and angles (°) for $[CoL_2]\cdot CH_2Cl_2$

N1-Co1	2.221(4)	O3-Co1	2.004(3)	O1-Co1	1.997(3)
N4-Co1	2.248(4)	N6-Co1	2.088(4)	N3-Co1	2.103(4)
O1-Co1-O3	96.04(14)	N6-Co1-N1	86.75(16)	N6-Co1-N3	159.13(15)
O1-Co1-N6	105.46(14)	N3-Co1-N1	78.02(16)	O1-Co1-N1	167.22(15)
O3-Co1-N6	89.91(14)	O1-Co1-N4	88.04(14)	O3-Co1-N1	87.59(15)
N6-Co1-N4	77.64(15)	O3-Co1-N4	167.54(14)	O1-Co1-N3	89.21(14)
N3-Co1-N4	88.33(15)	N1-Co1-N4	90.98(16)	O3-Co1-N3	103.46(14)

Table S5 Parameters of the O-H···Cl type interaction (Å, °) for $[CoL_2]\cdot CH_2Cl_2$

D-H…A	d(D…A)	d(H…A)	angle (D-H…A)
C(10)-H(10)…Cl'(1)	3.8280(56)	3.0331(26)	144.400(296)

Table S6 π-π stacking interactions involving Cg1(C15C16C17C18C19C20), Cg2 (C22C23C24C25C26C27), Cg3 (C1C2C3C4C5C6), Cg4 (C8C9C10C11C12C13), Cg5 (S2N5C16C15N4), Cg6 (S2N5C16C15N4)

π-π[a]	d(Cg-Cg)[b]	α[c]	Cg-plane[d]	Slip(Å)[e]	Symmetry[f]	Colour[g]
Cg1-Cg2	3.55	8.12	3.38/3.45	1.08/0.84	–*x*, 1–*y*, 1–*z*	pink
Cg3-Cg4	3.52	8.76	3.33/3.34	1.13/1.10	–*x*, –*y*, –*z*	blue
Cg5-Cg6	3.67	0.000	3.53	1.00	1–*x*, 1–*y*, 1–*z*	violet

[a]Distance between the centroids of the *I* and *Y* rings in Å; [b]Dihedral angle between the *I* and *Y* planes in degrees; [c]Perpendicular distance in Å of the centroid Cg(*I*) on the mean plane of the *Y* ring [d]Distance in Å between the centroid Cg(*I*) and perpendicular projection of the centroid Cg(*Y*) on the *I* ring; [f]Symmetry applied on the plane Cg(I) to obtain Cg(Y); [g]Colour used to distinguish intermolecular interactions (dotted lines) in Figure S7.

Ab initio calculations on the *zfs* tensor

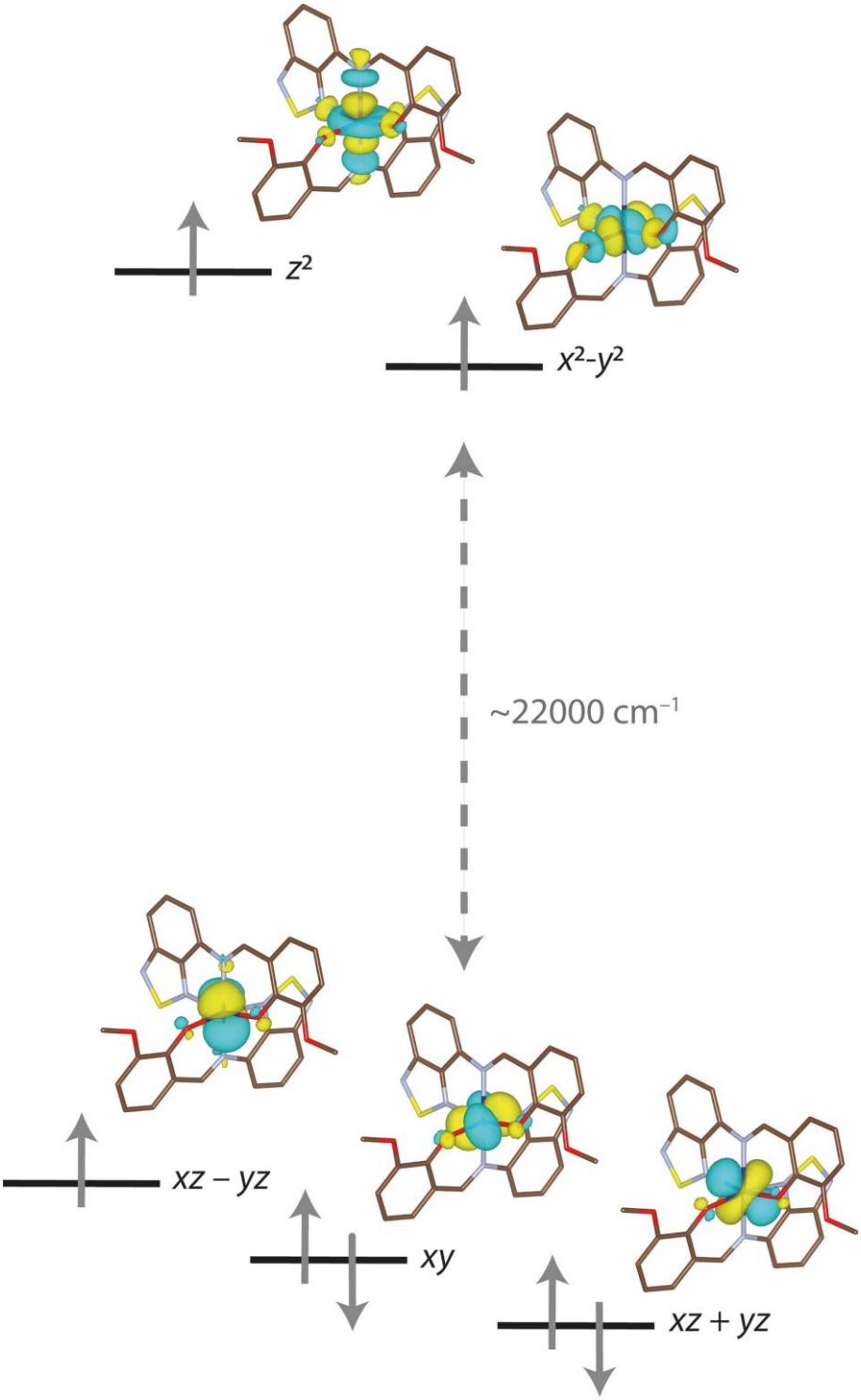

Fig. S8 Splitting of d orbitals and electronic configuration for the quartet ground state obtained from a CASSCF/NEVPT2 calculation on the experimental geometries of **1**. Molecular orbitals are displayed considering a cut-off equal to 0.01 e bohr^{-3}. Hydrogen atoms are omitted for clarity.

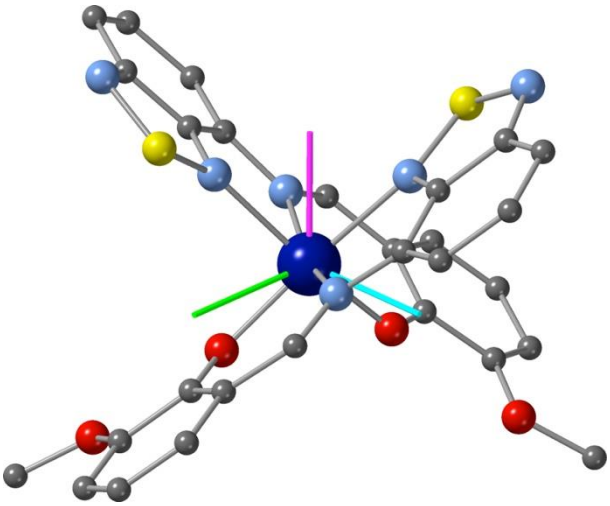

Fig. S9 Relative orientation of the experimental coordination sphere geometry of **1** and the calculated *D* tensor (*x* = cyan, *y* = green, *z* = magenta). Colour code: dark blue, cobalt; light blue, nitrogen; red, oxygen; grey, carbon; yellow, sulphur. Hydrogen atoms are omitted for clarity.

Table S7 Energy of the calculated quartet (Q_i) and triplet (D_i) excited states and their contributions to the *D* and *E* values for **1** obtained from CASSCF/NEVPT2 calculations. D_{SS} is the spin-spin contribution to axial *zfs* parameter, and D_Q and D_D are the sum of spin-orbit contributions coming from quartet and doublet excited states

Co1					Co2				
State	Energy[a]	*S*	D[a]	E[a]	State	Energy[a]	*S*	D[a]	E[a]
D_{SS}		4	+0.786	+0.238	D_5	19433.5	2	+2.693	+0.108
D_Q		4	–57.332	–14.859	D_6	19840.1	2	–0.176	+0.327
D_D		2	+4.943	+0.137	D_7	19933.0	2	–0.497	+0.580
Q_1	746.4	4	–77.962	–0.997	D_8	20476.7	2	–0.095	+0.173
Q_2	1970.6	4	+12.191	–15.096	D_9	22901.4	2	–1.413	–1.409
Q_3	8697.9	4	+2.953	–4.386	D_{10}	23505.8	2	+0.346	+0.102
Q_4	9100.6	4	+0.471	+0.581	D_{11}	23667.6	2	–0.095	+0.085
Q_5	10015.0	4	+5.064	+5.106	D_{12}	26142.5	2	–0.072	+0.061
Q_6	18075.2	4	+0.013	–0.015	D_{13}	28030.6	2	+0.412	–0.032
Q_7	21912.5	4	+0.014	–0.045	D_{14}	28815.4	2	–0.112	–0.145
Q_8	23113.1	4	–0.005	+0.002	D_{15}	29693.2	2	–0.414	+0.503
Q_9	23559.5	4	–0.071	–0.009	D_{16}	29726.4	2	–0.023	–0.017
D_1	11027.0	2	+4.767	+1.041	D_{17}	30130.7	2	–0.010	+0.005
D_2	12267.0	2	–1.093	–1.217	D_{18}	30577.6	2	+0.079	+0.198
D_3	18700.4	2	–0.001	+0.001	D_{19}	32313.5	2	–0.365	–0.349
D_4	18856.1	2	+0.034	–0.002	D_{20}	32430.2	2	+0.978	+0.124

[a]Values in cm^{-1}.

Magnetic measurements

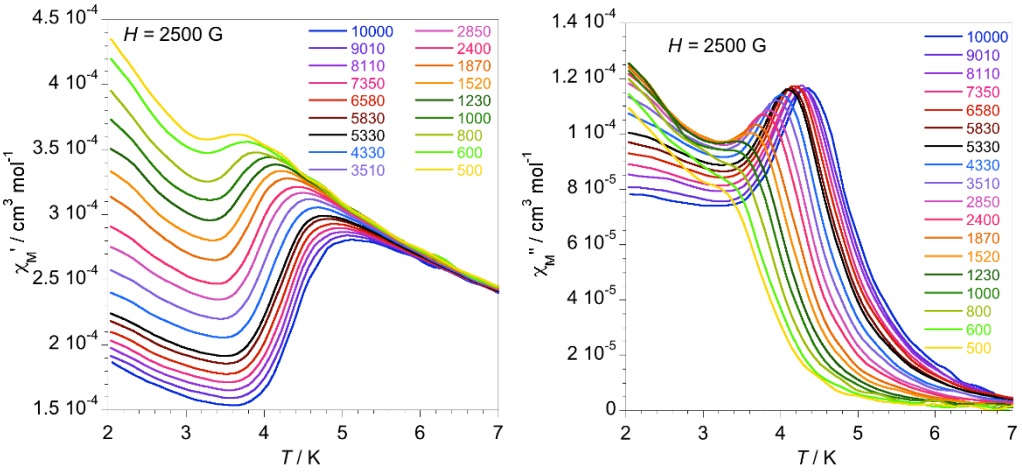

Fig. S10 Frequency dependence of the in-phase (left) and out-of-phase (right) components of the magnetic susceptibility of **1** under a static magnetic field H_{dc} = 2500 G with an oscillating field ±0.5 G and at the indicated frequencies

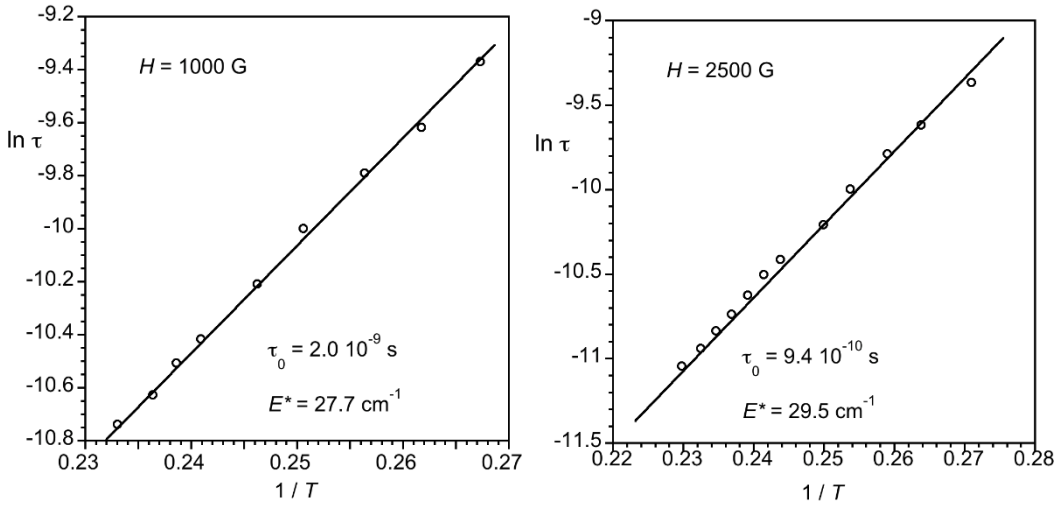

Fig. S11 Arrhenius plots in the form of ln (τ) as a function of 1/*T* for **1** under static magnetic field of 1000 (left) and 2500 (right): (o) experimental data; (—) fit by eq. (3).

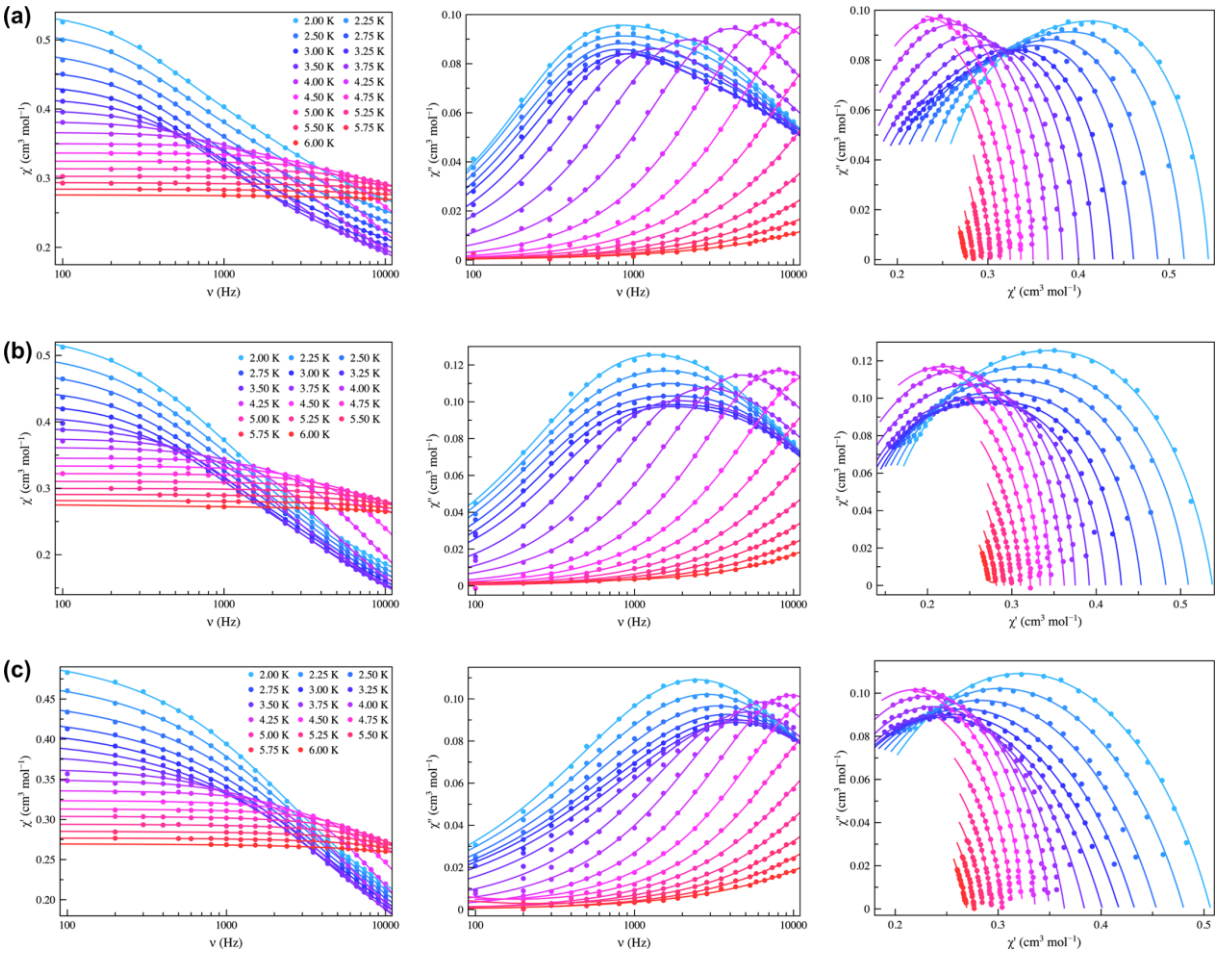

Fig. S12 Frequency dependence of χ_M' (left) and χ_M'' (middle), Cole-Cole plots (right) of **1** under applied *dc* static fields of 1.0 (a), 2.5 (b), and 5.0 kOe (c) with ± 0.005 kOe oscillating field in the temperature range 2.0–6.0 K (blue to red gradient). Solid lines are the best-fit curves simulated by using the generalized Debye model (see text).

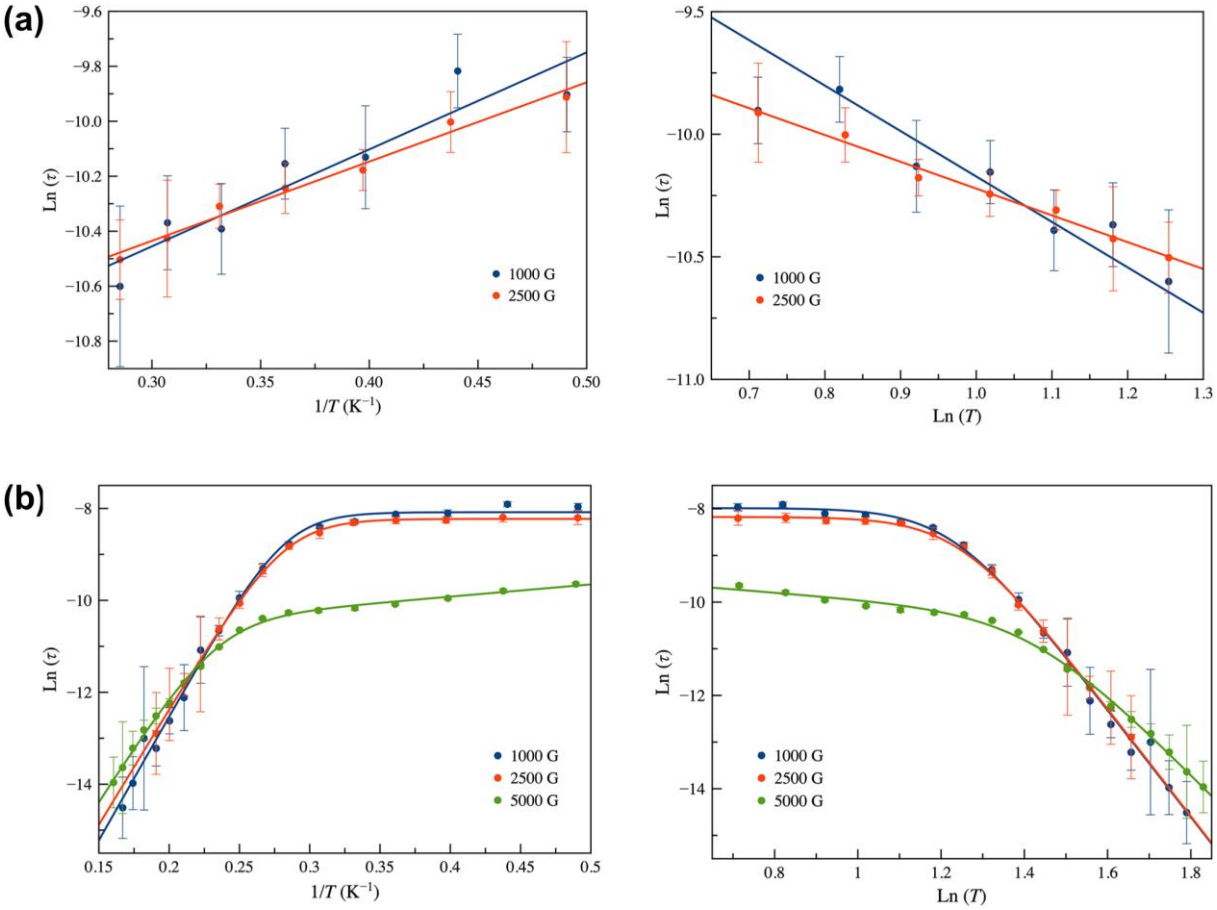

Fig. S13 Arrhenius (left) and ln(τ) *vs* ln(*T*) (right) plots for the calculated magnetic relaxation times (τ) of **1** under *dc* static fields of 1.0 (blue), 2.5 (red), and 5.0 kOe (green) for the two competing relaxation processes, one of them predominating at low temperatures (a) and other at higher ones (b). Standard deviations appear as vertical error bars. Solid lines are the best-fit curves simulated by combinations of quantum-tunnelling, Orbach and Raman mechanisms. More details are given in the main text.

Table S8 Selected fits of ac-magnetic data at different applied dc fields of **1** obtained from the Arrhenius plots

H_{dc}[a]	*Process*[b]	$\tau_{0,QT} \times 10^{4}$ [c]	$\tau_1 \times 10^{11}$ [c]	U_{eff1}[d]	$\tau_2 \times 10^{6}$ [c]	U_{eff2}[d]
1000	**HT**	3.1 ± 0.3	7 ± 3	37.5 ± 1.4		
	LT				10.0 ± 2.2	2.5 ± 0.4
2500	**HT**	2.67 ± 0.07	18 ± 4	35.0 ± 0.6		
	LT				12.3 ± 0.8	2.00 ± 0.12
5000	**HT**		42 ± 11	33.4 ± 1.0	17.1 ± 2.3	1.84 ± 0.24
	LT					

[a]Values in kOe; [b]Ocurring at high (HT) or low (LT) temperatures; [c,d]Values in cm^{-1}.

Table S9 Selected fits of ac-magnetic data at different applied dc fields of **1** obtained from the ln(τ) *vs* ln(*T*) plots

H_{dc}[a]	*Process*[b]	$\tau_{0,QT} \times 10^{4}$ [c]	$C_1 \times 10^{4}$ [c]	n_1	$C_2 \times 10^{-3}$ [c]	n_2
1000	**HT**	3.4 ± 0.3	22 ± 14	11.5 ± 0.4		
	LT				4.1 ± 1.0	1.85 ± 0.23
2500	**HT**	2.82 ± 0.11	20 ± 8	11.6 ± 0.3		
	LT				9.2 ± 0.5	1.09 ± 0.05
5000	**HT**		600 ± 40	9.2 ± 0.4	10.2 ± 2.1	0.71 ± 0.21
	LT					

[a]In kOe; [b]Ocurring at high (HT) or low (LT) temperatures; [c]In s^{-1} K^{-n}.

NMR spectra

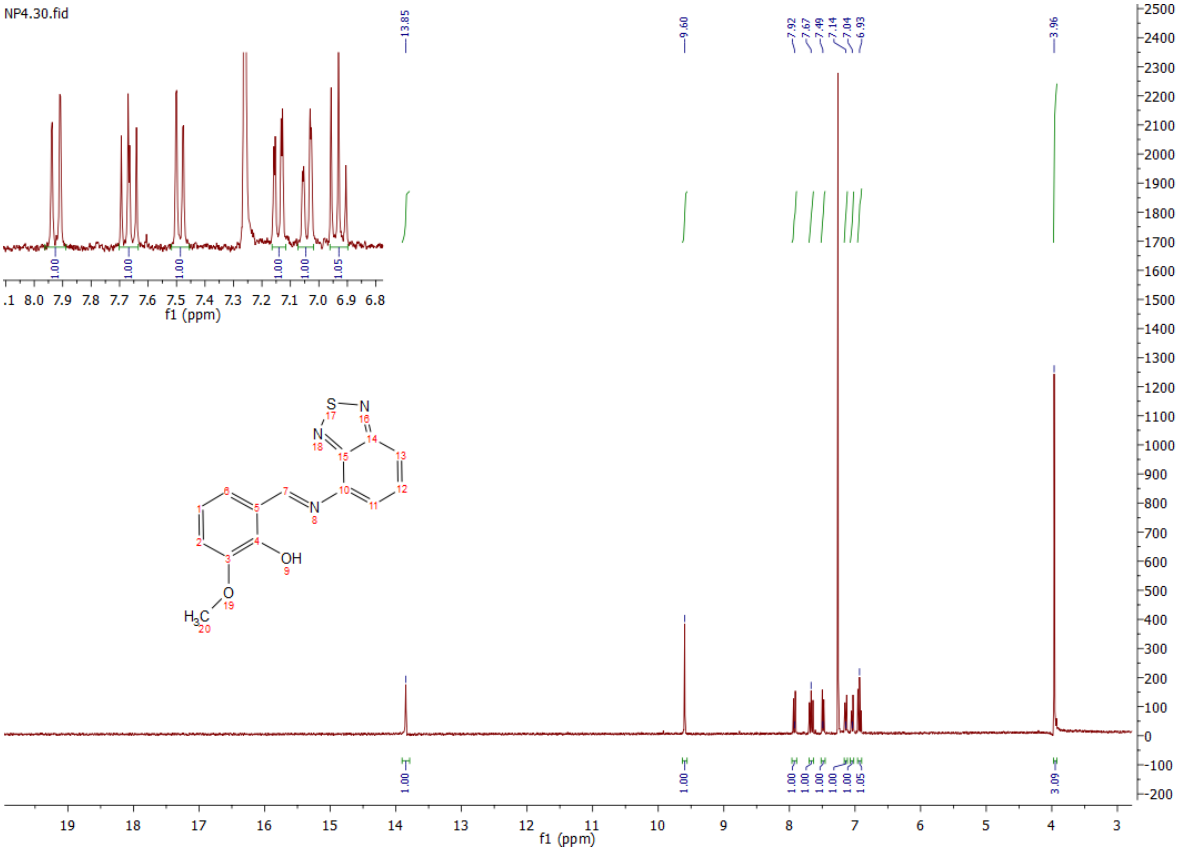

Fig. S14 ^{1}H NMR spectrum of compound HL in $CDCl_3$.

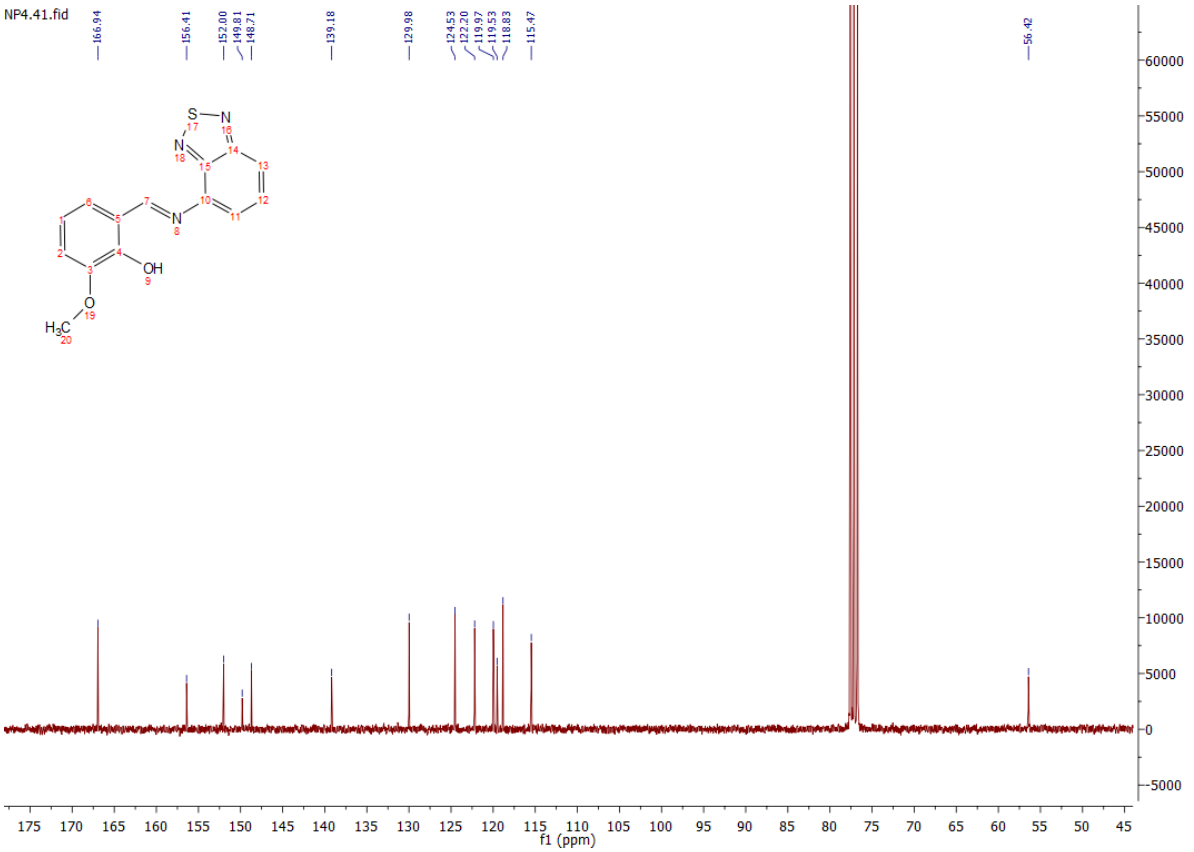

Fig. S15 ^{13}C NMR spectrum of compound HL in $CDCl_3$.

1 G. M. Sheldrick, *Programs for the Refinement of Crystal Structures,* ed. 1996.

2 L. Farrugia, *J. Appl. Crystallogr.*, 1999, **32**, 837.